Available online at www.sciencedirect.com
SCIENCE DIRECT
Geochimica et Cosmochimica Acta 70 (2006) 2790–2805
Geochimica
www.elsevier.com/locate/gca

Enhancement and inhibition of iron photoreduction by individual ligands in open ocean seawater

Micha J.A. Rijkenberg [a,b,*], Loes J.A. Gerringa [b], Vicky E. Carolus [b], Ilona Velzeboer [b], Hein J.W. de Baar [a,b]

[a] *Department of Marine Biology, University of Groningen, P.O. Box 14, 9750 AA Haren, The Netherlands*
[b] *Royal Netherlands Institute for Sea Research, P.O. Box 59, 1790 AB Den Burg, The Netherlands*

Received 13 December 2004; accepted in revised form 7 March 2006

Abstract

In laboratory experiments, we investigated the effect of five individual Fe-binding ligands: phaeophytin, ferrichrome, desferrioxamine B (DFOB), inositol hexaphosphate (phytic acid), and protoporphyrin IX (PPIX) on the Fe(II) photoproduction using seawater of the open Southern Ocean. Addition of 10–100 nM Fe(III) to open Southern Ocean seawater without the model ligands and containing; 1.1 nM dissolved Fe(III), 1.75 ± 0.28 equivalents of nM Fe of natural ligands with a conditional stability constant (log K') of 21.75 ± 0.34 and a concentration DOC of 86.8 ± 1.13 μM C leads to the formation of amorphous Fe(III) hydroxides. These amorphous Fe(III) hydroxides are the major source for the photoproduction of Fe(II). The addition of the model ligands changed the Fe(II) photoproduction considerably and in various ways. Phaeophytin showed higher Fe(II) photoproduction than ferrichrome and the control, i.e., amorphous Fe(III) hydroxides. Additions of phytic acid between 65 and 105 nM increased the concentration of photoproduced Fe(II) with 0.16 nM Fe(II) per nM phytic acid, presumably due to the co-aggregation of Fe(III) and phytic acid leading via an increasing colloidal surface to an increasing photoreducible Fe(III) fraction. DFOB and PPIX strongly decreased the photoproduced Fe(II) concentration. The low Fe(II) photoproduction with DFOB confirmed reported observations that Fe(III) complexed to DFOB is photo-stable. The PPIX hardly binds Fe(III) in the open Southern Ocean seawater but decreased the photoproduced Fe(II) concentration by complexing the Fe(II) with a binding rate constant of $k_{\mathrm{Fe(II)PPIX}} = 1.04 \times 10^{-4} \pm 1.53 \times 10^{-5}\ \mathrm{s^{-1}\ nM^{-1}}$ PPIX. Subsequently, PPIX is suggested to act as a photosensitizing producer of superoxide, thus increasing the dark reduction of Fe(III) to Fe(II). Our research shows that the photochemistry of Fe(III) and the resulting photoproduced Fe(II) concentration is strongly depending on the identity of the Fe-binding organic ligands and that a translation to natural conditions is not possible without further characterization of the natural occurring ligands.

1. Introduction

Iron is an important trace metal required in essential biochemical systems necessary to provide cells with the energy and biological components for growth and multiplication (Harrison and Morel, 1986; Rueter and Ades, 1987; Raven, 1990; Rueter et al., 1990; Greene et al., 1991; Geider and la Roche, 1994). Well known Fe-requiring cellular processes include photosynthesis and nitrogen fixation (Rueter and Ades, 1987; Geider et al., 1993). Iron is one of the important factors limiting primary production in large open oceanic areas such as the Northeast Pacific, the Equatorial Pacific, and the Southern Ocean (Martin and Fitzwater, 1988; de Baar et al., 1990; de Baar and Boyd, 2000; de Baar et al., 2005) and can be limiting in coastal areas as well (Hutchins and Bruland, 1998; Bruland et al., 2001; Strzepek and Harrison, 2004).

The chemistry of Fe in seawater is very complex. The Fe(III) and its hydrolysis products have very low solubility

* Corresponding author. Present address: School of Ocean and Earth Science, University of Southampton, National Oceanography Centre Southampton, SO14 3ZH Southampton, UK. Fax: +44 2380593059.
E-mail address: mzr@noc.soton.ac.uk (M.J.A. Rijkenberg).

0016-7037/$ - see front matter © 2006 Elsevier Inc. All rights reserved.
doi:10.1016/j.gca.2006.03.004

products resulting in a tendency to form particulate iron oxyhydroxides (Millero, 1998; Liu and Millero, 1999; Moffett, 2001; Waite, 2001; Liu and Millero, 2002). Organic complexation of Fe(III) in seawater increases the overall Fe solubility (Kuma et al., 1996; Johnson et al., 1997). Although organic Fe(III)-binding ligands are often found in excess over the dissolved Fe pool (Boyé et al., 2001), it does not prevent the existence of a colloidal Fe pool within the operational defined "dissolved" Fe fraction (all Fe passing through a 0.2 μm filter). Nishioka et al. (2005) distinguished the Fe pools by operational size discrimination among others in a particulate Fe (>0.2 μm), and a fine colloidal Fe pool (200 kDa–0.2 μm), and showed the importance of these Fe fractions in the Southern Ocean polar front between South Africa and Antarctica.

The Fe(II), although more soluble in seawater, becomes rapidly oxidized by O_2 and H_2O_2 (Millero et al., 1987; Millero and Sotolongo, 1989; King et al., 1995). Remarkably, significant and stable concentrations of Fe(II) have been determined in the Northeast Atlantic (Boyé et al., 2003), the East-equatorial Atlantic (Bowie et al., 2002), and during a Southern Ocean Fe enrichment experiment (Croot et al., 2001).

Redox reactions and physical/chemical speciation are shown to be important for the bioavailability of Fe for phytoplankton. The Fe(II) is assumed to be an Fe fraction suitable for biological uptake (Anderson and Morel, 1980, 1982; Takeda and Kamatani, 1989; Maldonado and Price, 2001). Furthermore, the wavelength-dependent Fe redox cycle initiated by photochemical processes is mentioned as an important mechanism by which (colloidal) Fe is converted into more reactive species (defined by the method applied) resulting in a presumably higher bioavailability to phytoplankton (Wells and Mayer, 1991; Johnson et al., 1994; Miller and Kester, 1994a; Rijkenberg et al., 2004).

Organic complexation can influence the redox speciation of Fe in seawater. Extensive literature on the influence of organic complexation of Fe on the oxidation kinetics is available (Theis and Singer, 1974; Millero et al., 1987; Voelker et al., 1997; Santana-Casiano et al., 2000; Moffett, 2001; Rose and Waite, 2002; Santana-Casiano et al., 2004). Organic compounds can also induce photoreductive dissolution of Fe from colloidal material (Waite and Morel, 1984; Waite et al., 1986; Waite and Torikov, 1987; Siffert and Sulzberger, 1991; Pehkonen et al., 1993, 1995; Sulzberger and Laubscher, 1995). Barbeau et al. (2001) have shown the photolysis of marine Fe(III)-siderophore complexes. The latter high-affinity Fe(III)-binding ligands secreted by e.g., marine bacteria to scavenge and transport Fe (Trick, 1989; Wilhelm and Trick, 1994; Granger and Price, 1999), may after photolysis lead to the formation of lower-affinity Fe(III) ligands and the reduction of Fe(III) to Fe(II). The ability of the Fe(III)-siderophore complex to be photoreduced was found to be strongly dependent on the Fe-binding functional group (Barbeau et al., 2003).

The identity, origin, and chemical characteristics of the organic Fe-binding ligands in the oceans are largely unknown. Despite differences in location and the method used a remarkably similar picture has emerged for the conditional stability constants of Fe ligand complexes. Values ranging between 10^{18} and 10^{23} have been measured in the North Atlantic (Gledhill and van den Berg, 1994; Wu and Luther, 1995; Witter and Luther, 1998), the North Sea (Gledhill et al., 1998), the Mediterranean Sea (van den Berg, 1995), the Arabian Sea (Witter et al., 2000b), the North Central and equatorial Pacific Ocean (Rue and Bruland, 1995, 1997), and the Southern Ocean (Nolting et al., 1998; Boyé et al., 2001, 2005). Witter et al. (2000a) conclude from comparisons between formation and dissociation rate constants of model ligands and field samples that most unknown ligands in seawater could originate from porphyrin and siderophore-like compounds. Macrellis et al. (2001) isolated organic Fe-binding ligands with hydroxamate and catecholate Fe-binding functional groups from the central California coastal upwelling system. Recently Gledhill et al. (2004) detected seven siderophore type compounds in coastal and near shore environments among which one was identified as DFOB (McCormack et al., 2003).

In the present study, the influence of Fe-binding ligands on the redox speciation of Fe in Southern Ocean seawater was investigated. The choice of model ligands to be investigated was based on their possible natural occurrence. Inspired by the article of Witter et al. (2000a), three Fe-chelating moieties were studied including: tetrapyrrole ligands (phaeophytin and PPIX), terrestrial and marine hydroxamate siderophores (ferrichrome and DFOB), and the terrestrial Fe-complexing storage ligand inositol hexaphosphate (phytic acid) (Fig. 1). The tetrapyrrole ligands were chosen to represent Fe-binding ligands derived from pigments such as chlorophyll-*a* released in the seawater upon cell lysis. Ferrichrome and DFOB (trihydroxamates from terrestrial microorganisms) were chosen to represent the structural types of siderophores that could be present in seawater (Macrellis et al., 2001; Martinez et al., 2001; Gledhill et al., 2004). Phytic acid is an organic phosphorous, metal-complexing (including Fe), storage compound abundant in seeds of terrestrial plants and has also been used as a terrestrial biomarker in coastal environments (Suzumura and Kamatani, 1995).

2. Materials and methods

2.1. Open Southern Ocean seawater

Clean Southern Ocean surface seawater (44°S 20°E, 30 November, 2000) was pumped into an over-pressurized class 100 clean air container using a Teflon diaphragm pump (Almatec A-15, Germany) driven by a compressor (Jun-Air, Denmark, model 600-4B) connected via acid-washed braided PVC tubing to a torpedo towed at approximately 2–3 m depth and at 5 m distance from the ship

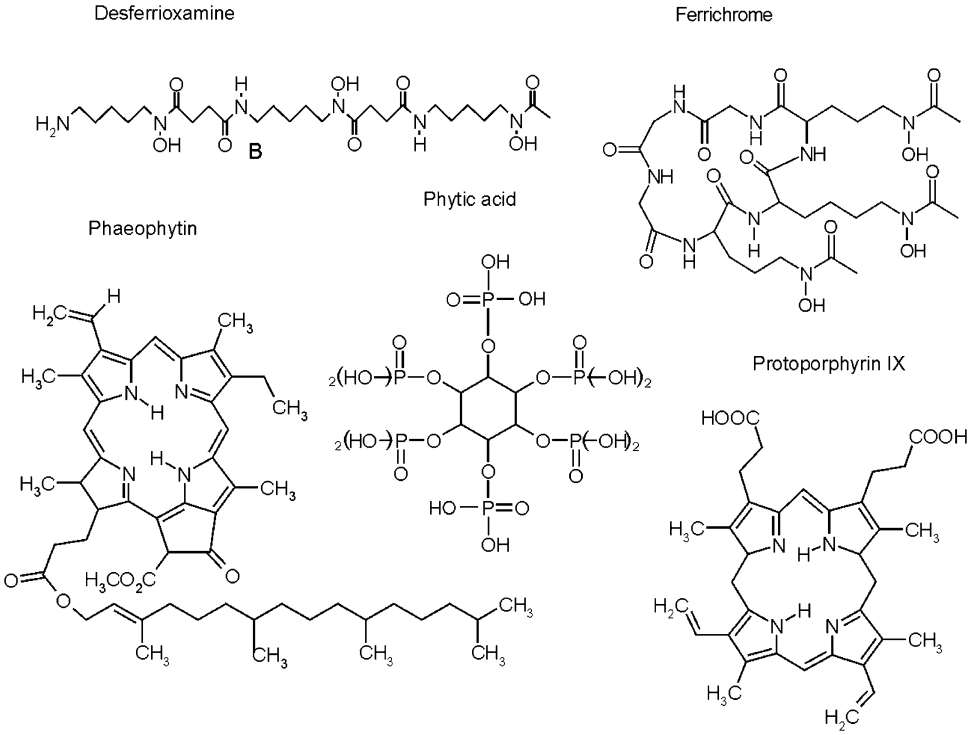

Fig. 1. The structure formulas for the Fe-binding ligands desferrioxamine B (DFOB), ferrichrome, phaeophytin, phytic acid, and protoporphyrin IX (PPIX).

(Polarstern, ANTXVIII/2). The seawater was filtered in-line by a filter with a cut-off of 0.2 μm (Sartorius Sartobran filter capsule 5231307H8). Upon return to the institute the tank was stored at room temperature. The collection of seawater into a large tank is prone to inadvertent slight contamination (Bowie et al., 2006). As we are adding 10–100 nM Fe(III) during our experiments (Table 1) we chose to use the slightly contaminated Southern Ocean seawater containing 1.1 nM dissolved Fe. Furthermore, the Southern Ocean seawater contained 1.75 ± 0.28 equivalents of nM Fe of natural ligands with a conditional stability constant (log K') of 21.75 ± 0.34 (given error shows the 95% confidence interval) as determined according to Croot and Johansson (2000) by Competitive Ligand Exchange-Adsorptive Cathodic Stripping Voltammetry (CLE-ACSV) with 2-(2-Thiazolylazo)-*p*-cresol (TAC) (10 μM) as competing ligand. The DOC concentration was 86.8 ± 1.13 μM C (given error is the standard deviation, $n = 3$). All seawater used in all experiments is the open Southern Ocean seawater from this one tank.

2.2. Reagents

All solutions were prepared using 18.2 MΩ nanopure water (MQ water) (Millipore). A 20 μM Fe(III) stock solution was made with ammonium Fe(III) sulphate ($NH_4Fe(III)(SO_4)_2 \cdot 12H_2O$, Baker Analyzed, reagent grade) in 0.012 M of 3x quartz distilled (3xQD) HCl. A 5.9×10^{-5} M PPIX (protoporphyrin IX disodium salt, Aldrich Chem.) stock solution, a 2.4×10^{-5} M DFOB (Novartis) stock solution, and a 8.7×10^{-5} M phytic acid (Aldrich Chem.) stock solution were used without further purification.

One milligram of chlorophyll-*a* (from spinach, Sigma) and ferrichrome (from *Ustilago sphaerogena*, Sigma) was deferrated using the method described by Witter et al. (2000a). The resulting phaeophytin and ferrichrome were finally resuspended in MQ water.

2.3. Light

Philips ultraviolet B (UVB: 280–315 nm) (TL-12), ultraviolet A (UVA: 315–400 nm) (TL' 40W/05), and visible light (VIS: 400–700 nm) (TL'D 36W/33) lamps were used to simulate the solar spectrum in the experiments (Fig. 2). Spectral conditions were measured using a MACAM Spectroradiometer SR9910 with a small spherical 4π sensor.

To prevent focussing effects during the experiments as well as the measurements of the irradiance spectra (from inside a polymethylmetacrylate (PMMA) bottle), all sides of the box-shaped UV transparent PMMA bottle ($11 \times 11 \times 11$ cm) (Steeneken et al., 1995), except the top, were covered with black plastic.

2.4. Fe(III) colloid formation

An acid cleaned 1 L Teflon bottle (Nalgene) was pre-equilibrated overnight with open Southern Ocean seawater containing 50 nM Fe(III) (15 °C, dark). The next day this

Table 1
Overview of the photochemical experiments in open Southern Ocean seawater including the irradiance of UVB, UVA, and VIS and the Fe(III) speciation

Fe(III) added (nM)	Ligand[a]	[Ligand] (nM)	[Fe(III)L_{model}][b] (nM)	[Fe(III)$L_{natural}$][c] (nM)	Fe′ (nM)	UVB[d] (Wm^{-2})	UVA[d] (Wm^{-2})	VIS[d] (Wm^{-2})
11	—	—	—	1.75	10.4	0.91	2.57	2.77
15	—	—	—	1.75	14.4	0.91	2.57	2.77
20	—	—	—	1.75	19.4	0.91	2.57	2.77
10	PPIX	20	10.7	0.36	4.6×10^{-4}	1.25	3.72	3.24
10	Phytic acid	20	10.7	0.43	5.7×10^{-4}	1.25	3.72	3.24
10	DFOB	20	10.1	0.10	2.6×10^{-3}	1.25	3.72	3.24
10	Phaeophytin	Excess	—	—	—	1.25	3.72	3.24
10	Ferrichrome	Excess	—	—	—	1.25	3.72	3.24
100	—	—	—	1.75	99.3	1.25	3.72	3.24
100	Phytic acid	80	80	1.75	19.3	1.25	3.72	3.24
100	Phytic acid	85	85	1.75	14.3	1.25	3.72	3.24
100	Phytic acid	90	90	1.75	9.3	1.25	3.72	3.24
100	Phytic acid	100	99.2	1.70	6.5×10^{-2}	1.25	3.72	3.24
100	Phytic acid	105	99.5	1.46	9.1×10^{-3}	1.25	3.72	3.24
100	Phytic acid	130	100	0.85	1.7×10^{-3}	1.25	3.72	3.24
100	Phytic acid	130	100	0.85	1.7×10^{-3}	1.25	3.72	3.24
100	PPIX	65	65	1.75	34.3	1.25	3.72	3.24
100	PPIX	85	85	1.75	14.3	1.25	3.72	3.24
100	PPIX	90	90	1.75	9.3	1.25	3.72	3.24
100	PPIX	100	99.3	1.69	5.3×10^{-2}	1.25	3.72	3.24
100	PPIX	130	100	0.75	1.3×10^{-3}	1.25	3.72	3.24
100	PPIX	130	100	0.75	1.3×10^{-3}	1.25	3.72	3.24

The Fe(III) speciation is calculated with an equilibrium complexation model (adapted from Gerringa et al. (2000)) and based on the presence of 1.1 nM dissolved Fe(III) and 1.75 equivalents of nM Fe(III) of natural ligands and the addition of varying concentrations Fe(III) and model ligands. The concentration inorganic Fe (Fe′) was calculated using the inorganic side reaction coefficient of Fe^{3+} (α) of 10^{10} (Millero, 1998).

[a] Addition of the ligand always preceded the addition of Fe(III) to the seawater.

[b] Conditional stability constants as reported by Witter et al. (2000a); $\log K'_{DFOB} = 21.6, \log K'_{phytic\ acid} = 22.3, \log K'_{PPIX} = 22.4$.

[c] Conditional stability constant as reported in this study; $\log K'_{natural\ L} = 21.75$.

[d] Reported irradiance data as measured from within the PMMA bottle.

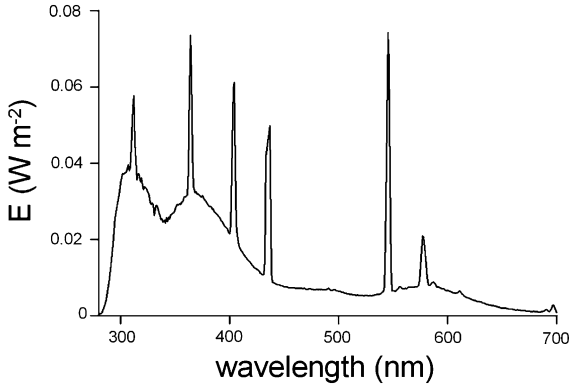

Fig. 2. A typical irradiance spectrum as measured from within the PMMA bottle used during the photochemical experiments. This spectrum was measured during the experiments where increasing concentrations Fe(III) were added to seawater. In comparison, the irradiance of UVB, UVA and VIS were 42%, 5.6%, and 6.1%, respectively, of the irradiance at noon of 13 May 2003 on Texel, the Netherlands.

water was discarded and the bottle refilled with 1 L seawater. Upon addition of 50 nM Fe(III) the colloid formation was measured as function of time (15 °C, dark). Subsamples were first purged with dry nitrogen gas to remove the oxygen during 170 s. Then the TAC (10 μM) and borate buffer (final pH 8.05, 5 mM) were added to the samples followed by 30 s purging and a deposition of the $Fe(TAC)_2$ complex at the mercury electrode during 60 s. At the end of the deposition period the potential was scanned using the differential pulse method. The Fe(III) labile to TAC was calculated from the stripping current (Croot and Johansson, 2000).

2.5. Photoreduction of Fe(III) with and without different organic Fe-binding ligands

All experiments were performed in an over-pressurized class 100 clean air, temperature controlled container laboratory using a temperature of 4 °C. Prior to use, PMMA bottles (1 L) were pre-equilibrated with Southern Ocean seawater (<0.2 μm filtered, pH 8.07 (Metrohm 713 pH meter), experimental volume of 500 ml, 4 °C, dark) containing the same concentration Fe(III) (range 10–100 nM) and ligand as used during the experiments.

An experiment typically started with measuring the background concentration Fe(II) in the dark, after which the lamps were switched on. During 60–90 min the concentration of Fe(II) was followed. Next, the oxidation of Fe(II) was followed for 30 min after turning off the light. The seawater solution was continuously stirred using a Teflon stirring bean. The experiments are summarized in Table 1.

2.6. Iron(II) analysis

Concentrations of Fe(II) were followed using an automated flow injection analysis system employing a luminol-based chemiluminescence detection of Fe(II) (King et al., 1995). An alkaline luminol solution (50 μM luminol in 0.5 M NH_3 (suprapur, Merck) and 0.1 M HCl (suprapur, Merck)) is mixed with the sample in a flow cell in front of a Hamamatsu HC135 photon counter. At pH 10, Fe(II) is rapidly oxidized by oxygen on a millisecond time scale causing the oxidation of luminol, producing blue light (Xiao et al., 2002). Every 93 s a sample was transported in-line from the PMMA bottle into the flow cell using a MQ water carrier. The complete analysis system, reagents and tubing, was kept in the dark.

Calibration was performed by standard addition to the sample matrix. The 0.01 M Fe(II) stock was prepared monthly by dissolving ferrous ammonium sulfate hexahydrate ($Fe^{(II)}(NH_4SO_4)_2 \cdot 6H_2O$, Baker Analyzed, reagent grade) in 0.012 M of 3xQD HCl. Working solutions were prepared daily. All Fe(II) stock solutions were refrigerated in the dark at 4 °C if not in use.

The time delay between Fe(II) addition and measurement caused oxidation. This oxidation was accounted for by extrapolating the data back to time zero because Fe(II) oxidation in seawater approximates pseudo-first-order kinetics.

2.7. Total dissolved Fe analysis

Dissolved iron, defined as the Fe fraction passing a 0.2 μm filter, was determined using flow injection analysis with luminol chemiluminescence and H_2O_2 (de Jong et al., 1998).

2.8. Hydrogen peroxide analysis

Hydrogenperoxide (H_2O_2) was measured after Gerringa et al. (2004) by fluorescence (Waters fluorometer, type 470) after enzyme-catalyzed dimerisation of (*p*-hydroxyphenyl) acetic acid (POHPAA) (Miller and Kester, 1988, 1994b).

2.9. Binding of Fe(III) and Fe(II) by PPIX

To investigate binding of Fe(III) by PPIX, increasing concentrations PPIX (0–125 nM) and 10 μM of the competing ligand TAC were added to 8 Teflon cups with open Southern Ocean seawater after which 15 nM Fe(III) was added to the 8 Teflon cups, and next equilibrated during >12 h. Then the concentration $Fe(TAC)_2$ (TAC-labile Fe(III)) in the samples was measured using CLE-ACSV (Croot and Johansson, 2000).

To investigate the binding of Fe(II), we used a 1.0×10^{-7} M Fe(II) stock solution in 0.012 M (3xQD) HCl and a 2.58×10^{-5} M PPIX stock solution in MQ water. The experiments were performed at 15 °C in a low light environment without UV, such that no photoproduction of Fe(II) was observed. The Fe(II) (final concentration 1 nM) and PPIX (final concentration 25, 50, or 100 nM) were simultaneously added to open Southern Ocean seawater. The Fe(II) concentration was measured using FIA based on luminol chemiluminescence (see above). The presence of PPIX did not influence the luminol reaction with the samples in the flow cell as no change in signal was observed after addition of PPIX to the luminol reagent. We corrected for the slow decrease in the concentration of Fe(II) of the standard solution due to slow oxidation with 0.064 nM h^{-1} ($R^2 = 0.98$, $n = 8$).

Calculation shows that H_2O_2 eventually present in the stock solution can only have a very small influence on the determination of the $k_{Fe(II)PPIX}$. We assumed for example the realistic concentrations of 5 and 10 nM H_2O_2 for, respectively, the seawater and the stock solution. In a worst case scenario H_2O_2 is responsible for all Fe(II) oxidation (k_{ox} is $2.53 \times 10^{-3} \pm 6.2 \times 10^{-5}$ in our experiments) when no PPIX is present. An addition of 100 μl stock solution without PPIX to 25 ml seawater results in an increase of 0.8% in Fe(II) oxidation. When we assume 20 nM H_2O_2 in the stock solution the Fe(II) oxidation increases with 1.6%. The binding of Fe(II) by PPIX using the $k_{Fe(II)PPIX}$ (as reported below) results in an increase of Fe(II) disappearance of 82%.

3. Results and discussion

3.1. Inorganic Fe(III) photoreduction

To understand the influence of organic Fe-binding ligands on the photo-induced Fe redox speciation in seawater, it is necessary to know how the photo-induced Fe redox processes act when Fe(III) is added to seawater in excess of the low concentration of natural organic ligands. Little is known about the crystalline forms of the Fe species formed upon the addition of a low concentration of Fe(III) to seawater. Based on model studies Moffett (2001) suggested that excess Fe(III) in aqueous alkaline media polymerizes into amorphous Fe(III) hydroxides. With ageing, these solids lose water and develop crystalline structures leading to two principal products, an amorphous solid, ferrihydrite ($Fe_5HO_8 \cdot 4H_2O$) (Schwertmann and Thalmann, 1976) also called marine ferrihydrite (Wells and Trick, 2004), and a more crystalline form lepidocrocite (γ-FeOOH) (Tipping et al., 1989). Ultimately these oxyhydroxide minerals will lose more water with ageing, and turn into more refractory minerals as hematite (α-Fe_2O_3) and goethite (α-FeOOH) (Schwertmann and Taylor, 1972; Schwertmann and Fischer, 1973; Cornell and Schwertmann, 1996). The formation of Fe(III) colloids (after a 50 nM Fe(III) addition to seawater) is fast and reaches equilibrium within 1.5–2 h (Fig. 3) as shown by the decrease in Fe concentration able to be bound by TAC within 90 s.

The Fe(II) concentration versus time in a photochemical experiment, typically resulting from an addition of Fe(III) to seawater, is shown in Fig. 4. To interpret the photo-

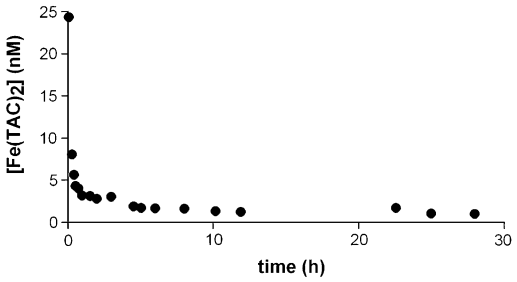

Fig. 3. The Fe colloid formation after the addition of 50 nM Fe(III) was visualized by the decrease in TAC-labile Fe ($Fe(TAC)_2$) with time.

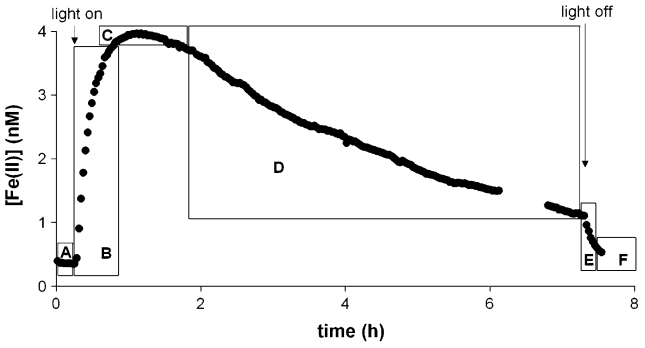

Fig. 4. The concentration of Fe(II) as a result of the irradiation of colloidal Fe (100 nM Fe(III) addition) in seawater. The typical characteristics used to compare the photochemical experiments were: (A) the constant concentration of Fe(II) in the dark before illumination (InStSDark Fe(II)); (B) the rapid increase of Fe(II) after starting irradiation with an initial Fe(II) photoproduction rate (InPrRate Fe(II)); (C) the decrease in the Fe(II) photoproduction rate reaching a maximum Fe(II) concentration (Max Fe(II)), this followed by (D) the decrease of the concentration Fe(II) during irradiance towards an steady state (StSLight Fe(II)); and (E) turning off the light resulted in a sharp decline due to the oxidation of Fe(II) to Fe(III) (Ox Fe(II)), resulting in (F) steady state of the Fe(II) concentration in the dark (FinStSDark Fe(II)).

chemical experiments several characteristics in the pattern of Fe(II) concentration versus time were used. The concentration of Fe(II) in the dark, prior to the irradiance treatment, was constant (Initial Steady State in the Dark of the concentration Fe(II), InStSDark Fe(II)) (Fig. 4, section A). In the dark other processes than photo(induced) reduction of Fe(III) are responsible for InStSDark Fe(II) such as thermal reduction (Hudson et al., 1992; Pullin and Cabaniss, 2003) or enzymatic Fe(III) reduction (Maldonado and Price, 2000). Although we cannot guarantee total sterile conditions, we assume that the role of external or internal bacterial enzymes was negligible or non-existent in our 0.2 μm filtered seawater.

Irradiance resulted in a rapid increase of the concentration of Fe(II). Several photo(induced) reduction mechanisms could be responsible for this increase: (i) the photoreduction of inorganic Fe oxyhydroxides (Wells and Mayer, 1991), (ii) a ligand to metal charge transfer (LMCT) reaction where an organic molecule is oxidized and Fe(III) is reduced (Kuma et al., 1995), and (iii) photo-induced reduction of Fe(III) via the oxygen radical superoxide O_2^- (Voelker and Sedlak, 1995). The initial Fe(II) photoproduction rate (Initial photoProduction Rate of Fe(II), InPrRate Fe(II)) was used to compare the different photochemical experiments (Fig. 4, section B). This InPrRate Fe(II) was calculated by modeling the concentration of InStSDark Fe(II) and the increase in the Fe(II) concentration during the first half hour of the irradiance treatment. The intercept of both lines, the exact time at which the irradiance treatment started, filled in the derivative of the previously modeled function resulted in the InPrRate Fe(II) (Rijkenberg et al., 2004).

The Fe(II) photoproduction rate decreased, leading to a maximum (Maximum Fe(II) concentration, Max Fe(II)) (Fig. 4, section C). The maximal photoproduced Fe(II) concentration was calculated by subtracting the initial Fe(II) steady state in the dark from the Fe(II) maximum (Maximum Produced Fe(II) concentration, MaxProd Fe(II)). After reaching this maximum the concentration of Fe(II) decreased slowly and reached a steady state (Steady State in the Light of the concentration Fe(II), StSLight Fe(II)) (Fig. 4, section D). The rapid increase to a maximum followed by a slow decrease in the Fe(II) concentration has been reported before from experiments with inorganic Fe colloids (Waite and Morel, 1984; Wells and Mayer, 1991). Wells and Mayer (1991) found that the photo-conversion rates diminished with continued irradiation when ferrihydrite was irradiated. One explanation for the decreasing Fe(II) concentrations during irradiance could be an increase in the oxidation rate. In all our experiments, the first order rate constants for oxidation in the light (k_2) are higher than the first order rate constants for oxidation in the dark (k_2') (Table 2). An additional explanation is a limited and decreasing availability of photoreducible Fe(III) (Rijkenberg et al., 2005). Emmenegger et al. (2001) found similar behavior of the concentration of Fe(II) with time after UV digestion of Swiss lake water destroying the organic material, thereby confirming that the observed pattern is typical for colloidal Fe(III) and independent of strong Fe-complexing organic chromophoric molecules. In addition, Waite and Morel (1984) have shown that the addition of excess amounts of the chromophore citrate did not influence this effect. Wells and Mayer (1991) suggested several possible mechanisms for the decreasing photoreduction rate with time, among which: (i) photoreduction becomes inhibited if residues from the photo-oxidation of chromophores accumulated on colloid surfaces over time, shielding active sites from further photoreaction, (ii) photoreduction becomes inhibited by the retention of photoreduced Fe(II) at the surface, or the rapid resorption of the re-oxidized Fe(III) species back onto the original surface. In either case, a shell of rapid-cycling labile Fe might form on the oxyhydroxide surface upon prolonged photolysis, upon which a third mechanism, (iii) progressive photochemical alterations of the oxyhydroxide surface would decrease its charge trapping efficiency, resulting in more charge migration into the crystal lattice.

Table 2
Experimental results from the experiments with increasing concentration Fe(III) to seawater, for five ligands and control, and for the experiments in which increasing concentrations of two model ligands (phytic acid and PPIX) were added to seawater containing 100 nM Fe(III)

Experiment	Ligand added (nM)	Fe(III) added (nM)	InStSDark Fe(II) (nM)	InPrRate Fe(II) (nM/h)	Max Fe(II) (nM)	Ox Fe(II)[a] (nM/h)	k_2'[b] (h^{-1})	k_2[c] (h^{-1})	FinStSDark Fe(II) (nM)	MaxProd Fe(II) (nM)
Southern Ocean sw.										
sw.	—	11	0.063 ± 0.0024	1.52	0.31 ± 0.0048	0.78	2.56	4.90	0.084 ± 0.0046	0.25
sw.	—	15	0.065 ± 0.0023	2.62	0.55 ± 0.0038	1.35	2.46	4.76	0.11 ± 0.011	0.49
sw.	—	20	0.071 ± 0.0027	3.84	0.86 ± 0.0080	1.78	2.07	4.47	0.14 ± 0.027	0.81
No ligand	—	10	0.05 ± 0.01	3.81	0.48 ± 0.03	1.10	2.29	7.93	—	0.43
PPIX	20	10	0.04 ± 0.01	4.48	0.25 ± 0.01	1.28	5.12	17.92	0.095 ± 0.002	0.22
Phytic acid	20	10	0.08 ± 0.003	3.64	0.53 ± 0.01	0.89	1.68	6.87	—	0.45
DFOB	20	10	0.07 ± 0.01	3.13	0.15 ± 0.003	0.91	6.07	20.87	—	0.08
Phaeophytin	20	10	0.05 ± 0.01	3.29	0.58 ± 0.005	2.63	4.53	5.67	0.29 ± 0.007	0.53
Ferrichrome	20	10	0.06 ± 0.01	2.71	0.49 ± 0.008	1.77	3.61	5.53	0.13 ± 0.008	0.43
Phytic acid	80	100	0.023 ± 0.0064	16.68	4.54 ± 0.056	10.99	2.42	3.67	0.64 ± 0.024	4.52
Phytic acid	85	100	0.060 ± 0.0041	15.93	5.23 ± 0.023	10.21	1.95	3.05	0.77 ± 0.054	5.17
Phytic acid	90	100	0.176 ± 0.0077	17.08	6.05 ± 0.011	11.13	1.83	2.82	1.72 ± 0.041	5.87
Phytic acid	100	100	0.225 ± 0.0034	20.50	7.60 ± 0.004	7.78	1.02	2.70	1.77 ± 0.055	7.37
Phytic acid	105	100	0.422 ± 0.0029	44.78	9.15 ± 0.036	9.57	1.05	4.89	—	8.72
Phytic acid	130	100	0.286 ± 0.0054	32.56	5.91 ± 0.012	11.13	1.88	5.51	1.48 ± 0.046	5.62
Phytic acid	130	100	0.576 ± 0.0072	23.46	6.05 ± 0.022	8.10	1.34	3.88	1.37 ± 0.079	5.47
									slope (nM/h)	
PPIX	65	100	0.21 ± 0.0012	11.31	—	3.31	—	—	0.069	—
PPIX	85	100	0.24 ± 0.0045	4.31	—	2.04	—	—	0.037	—
PPIX	90	100	0.24 ± 0.0027	4.84	—	4.74	—	—	0.065	—
PPIX	100	100	0.23 ± 0.0020	4.05	—	4.12	—	—	0.048	—
PPIX	130	100	0.23 ± 0.0016	5.47	—	4.35	—	—	0.024	—
PPIX	130	100	0.31 ± 0.0006	7.02	—	9.87	—	—	0.12	—

The initial steady state in the dark of the concentration Fe(II) (InStSDark Fe(II)), initial photoproduction rate of Fe(II) (InPrRate Fe(II)), the maximum Fe(II) concentration (Max Fe(II)), the oxidation of Fe(II) in the dark (Ox Fe(II)), the final steady state in the dark of the concentration Fe(II) (FinStSDark Fe(II)), and the maximum produced Fe(II) concentration (MaxProd Fe(II)) are shown. The standard errors for FinStSDark Fe(II) are from the mathematical fit of the data points. The standard errors for InStSDark and Max Fe(II) are calculated as the standard error from the average of at least 3 data points.

[a] The oxidation data were mathematically described by a first order function. The numbers given are the Fe(II) oxidation rates at the moment of turning off the light.

[b] k_2' is the first order rate constant for Fe(II) oxidation in the dark: d[Fe(II)] = Max Fe(II) − FinStSDark Fe(II), t = d[Fe(II)]/Ox Fe(II), $k_2' = (\mathrm{d[Fe(II)]}/t)/\text{Max Fe(II)}$.

[c] k_2 is the first order rate constant for Fe(II) oxidation in the light: $\mathrm{d[Fe(II)]}/\mathrm{d}t = k_1 - k_2\,[\mathrm{Fe(II)}]$, k_1 is InPrRate Fe(II), at "steady state" (Max Fe(II)) the Fe(II) production and consumption rates are equal and $[\mathrm{Fe(II)}] = k_1/k_2$.

The main process remaining, in the post illumination period, is the oxidation of Fe(II) to Fe(III) by O_2 and H_2O_2 (Oxidation of Fe(II), Ox Fe(II)) (Millero et al., 1987; Millero and Sotolongo, 1989; King et al., 1995) (Fig. 4, section E). The rapid oxidation of Fe(II) in the dark resulted in a steady state of the Fe(II) concentration in the dark (Final Steady State in the Dark of the concentration Fe(II), FinStSDark Fe(II)) (Fig. 4, section F).

Increasing concentrations of Fe(III) were added to the seawater to investigate whether more Fe(II) is photoproduced and how this affects the photochemical characteristics. Addition of Fe(III) indeed led to an increase in the photoreducible Fe(III) fraction and subsequent to more photoproduced Fe(II) (Fig. 5). With increasing concentrations of Fe(III) a linear increase in the InPrRate Fe(II) with a slope of 0.257 ± 0.009 and a linear increase in the MaxProd Fe(II) with a slope of 0.062 ± 0.001 were observed (both relations with a R^2 of 0.999, $n = 3$) (Table 2). The excellent linear relationship between the added Fe(III) concentration and the experimental characteristics as InPrRate Fe(II) and MaxProd Fe(II) showed that ageing of the colloids during the time-span of the experiments (one day) did not influence the results. Since the additions of Fe(III) to the seawater exceeded the free strong organic Fe-binding ligand concentration and the solubility product of Fe(III), amorphous Fe(III) hydroxides are apparently the main source for photoproduction of Fe(II) in our experiments. As a consequence, an influence of the added organic Fe-binding ligands on the formation of amorphous Fe(III) hydroxides will have an effect on the photoproduced Fe(II) concentration.

3.2. The influence of organic model ligands on the photochemistry of Fe(III) in seawater

The addition of organic model ligands could influence the photoproduction of Fe(II) in several ways: (i) by photo-induced Fe(III) reduction via a LMCT reaction, (ii) by

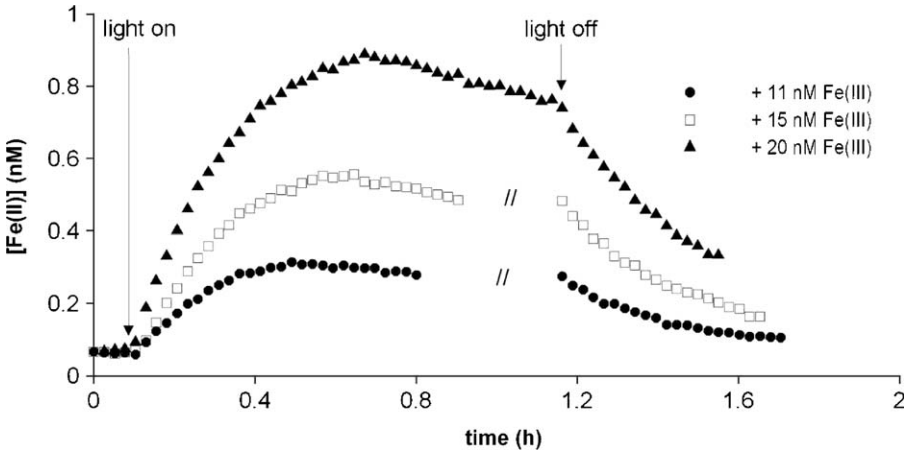

Fig. 5. The concentration of Fe(II) as a result of the irradiation of amorphous Fe(III) hydroxides produced by the addition of 11, 15, and 20 nM Fe(III) to seawater.

decreasing the inorganic Fe(III) concentration and subsequently decreasing the formation of Fe colloids, (iii) by modification of the colloid surface due to binding or adsorption to surface iron, or (iv) by influencing the overall structure of the iron colloids due to the precipitation of Fe(III)-organic solids. Furthermore, organic ligands may inhibit (Theis and Singer, 1974), accelerate or decelerate (Santana-Casiano et al., 2000, 2004) the oxidation of the photoproduced Fe(II).

The InPrRate Fe(II) decreased due to the addition of model ligands as follows: PPIX (4.48 nM h^{-1}) > no ligand ⩾ phytic acid > phaeophytin ⩾ DFOB > ferrichrome (2.71 nM h^{-1}) (Figs. 6A and B; Table 2).

The MaxProd Fe(II) concentration appeared slightly higher with phaeophytin and phytic acid in comparison with the control, although this was not confirmed by the InPrRate Fe(II) (Fig. 6A, Table 2). The DFOB and PPIX clearly affected the Fe(II) photoproduction in seawater

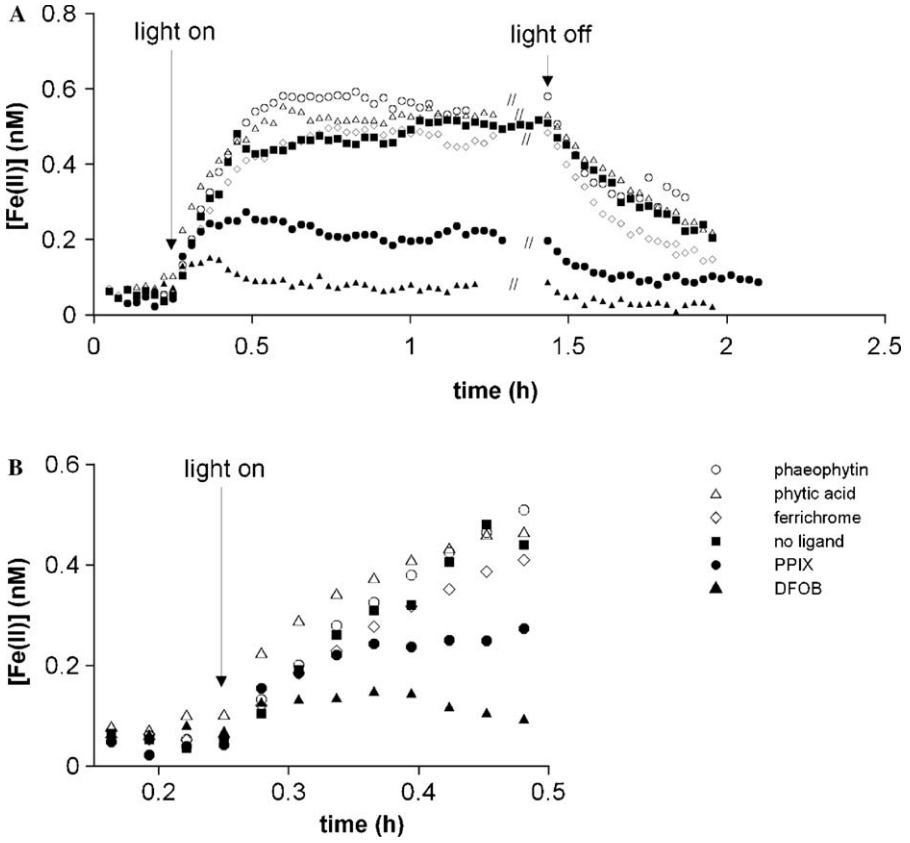

Fig. 6. (A) The photoproduction of Fe(II) after a 10 nM Fe(III) addition to seawater in the presence of PPIX (20 nM), phytic acid (20 nM), DFOB (20 nM), ferrichrome (excess), phaeophytin (excess), and control seawater without added Fe-binding ligands. (B) Focus on the time interval 0.15–0.5 h.

(Fig. 6A, Table 2). The Fe(III) complexed by DFOB is known to be completely photo-stable (Kunkely and Vogler, 2001). The fast Fe(III) complexation by DFOB decreases the colloidal Fe(III) fraction and thus decreases the photoproduction of Fe(II). Remarkably, for PPIX the MaxProd Fe(II) was found to be lower compared to the other ligands, although the InPrRate Fe(II) was clearly the highest. To explain the difference in effect between the two trihydroxamate siderophores ferrichrome and DFOB further experiments are necessary. The difference in effect between the two tetrapyrroles phaeophytin and PPIX could be the result of differences in solubility between PPIX and phaeophytin. Phaeophytin contains a large apolar phytol chain. Overall, these experiments show that the photoproduction of Fe(II) is strongly dependent on the individual organic Fe-binding ligand which is present.

In order to understand how phytic acid and PPIX, respectively, increased and decreased the Fe(II) photoproduction, these two ligands were studied in more detail.

3.2.1. Phytic acid

Irradiance of seawater containing 100 nM Fe(III) and concentrations of phytic acid in the range of 80–130 nM resulted in increasing photoproduction of Fe(II) compared to the control without ligands (Figs. 7A and B). The results showed a pattern of a fast increase until a maximum Fe(II) concentration. Using 105 nM phytic acid the maximum Fe(II) concentration was followed by a decrease in the Fe(II) concentration during irradiance which is similar to the observations with amorphous Fe(III) hydroxides (Fig. 4). This similarity in pattern, also observed in other experiments with phytic acid during longer irradiance (results not shown), has been observed before for colloidal Fe. We assume that this means that we observed the reduction of Fe(III) originating from a colloidal Fe pool (Wells and Mayer, 1991; Emmenegger et al., 2001). When the photoreducible colloidal Fe pool is only depending on the presence of free Fe(III) or in case Fe(III)-phytic acid is photoreactive we would expect to see a relation between InPrRate Fe(II) with increasing phytic acid concentration. Yet, no relationship between the InPrRate Fe(II) and the concentration of added phytic acid was found (Table 2) confirming that Fe(III) bound by phytic acid is not photolabile (Maldonado et al., 2005). However, the concentration MaxProd Fe(II) showed a linear relationship with the phytic acid concentration in the range 80–105 nM phytic acid (Fig. 8). For every nM phytic acid added an increase in the concentration MaxProd Fe(II) of 0.16 nM ($R^2 = 0.99$, $n = 5$) was observed. In contrast, the MaxProd Fe(II) of duplicate experiments with 130 nM phytic acid did not comply with the linear relationship and was lower.

The linear relationship between the concentration MaxProd Fe(II) and the concentration phytic acid might be explained by processes occurring when phytic acid and Fe(III) were added to seawater. Upon the addition of 100 nM Fe(III) to seawater containing phytic acid in concentrations ranging between 80 and 130 nM three processes are conceivable: (i) the hydrolysis and precipitation of Fe(III), forming colloids (Moffett, 2001), (ii) the binding and precipitation of Fe(III) by phytic acid (Anderson, 1963), and (iii) the adsorption of phytic acid to the Fe(III) containing aggregates (Ognalaga et al., 1994; Celi et al., 2003). The presence of six phosphate groups in the phytic acid molecules allowed different arrangements of the Fe(III) and phytic acid molecules. The combination of these processes will result in undefined aggregates of Fe(III) and phytic acid.

Anderson (1963) showed that precipitation of ferric phytic acid increased with a decreasing Fe(III) to P ratio, with increasing pH, and with increasing salinity. Moreover, phosphate can further disperse the already irregular surface of aggregates of amorphous Fe(III) oxyhydroxides (Parfitt, 1989) and present a larger surface for interaction with the environment, as for example for the photoproduction of Fe(II). If the same process occurs with phytic acid the aggregates will become more amorphous with an increasing concentration of phytic acid, thereby explaining the observation that more photo-reducible Fe(III) is formed with increasing concentrations of phytic acid (Fig. 8). A possible explanation of the lower concentration MaxProd Fe(II) observed after addition of 130 nM phytic acid could be the adsorption of the excess phytic acid to the surface of the ferric phytic acid aggregates decreasing the available photoreducible Fe(III) fraction.

Information on the complexation of Fe by phytic acid in seawater is limited to the conditional stability constant ($\log K'_{\mathrm{Fe3+L}} = 22.3$) and the Fe-phytic acid coordination ($\pm$2:1) in seawater with a pH of 6.9 (Witter et al., 2000a). Our study shows that phytic acid, until a certain concentration which is depending on the Fe(III) concentration, will substantially increase the size of the photoreducible Fe(III) fraction, probably via the formation of more amorphous ferric phytic acid aggregates.

3.2.2. Protoporphyrin IX

Addition of PPIX caused a dramatic decline in the photoproduced concentration of Fe(II) in the seawater (Figs. 7A and C). The different experimental characteristics did not show any relationship with the concentration of PPIX. This raised the question whether or not PPIX actually binds Fe(III).

Rue and Bruland (1995) and Witter et al. (2000a) determined a log K' for PPIX of 22.0 and 22.4, respectively, by titrating low concentrations of 0.9 and 2.5 nM PPIX, respectively, with Fe(III) in UV treated seawater. In this study Fe(III) was titrated with increasing concentrations PPIX resulting in a small decrease of 2.5 nM TAC-labile Fe(III) between 0 and 30 nM PPIX (Fig. 9). There was no substantial decrease in TAC-labile Fe(III) with increasing PPIX concentrations, thus only slight evidence for binding of Fe(III) by PPIX was found in our experiments. Questions were raised about the possibility that PPIX does

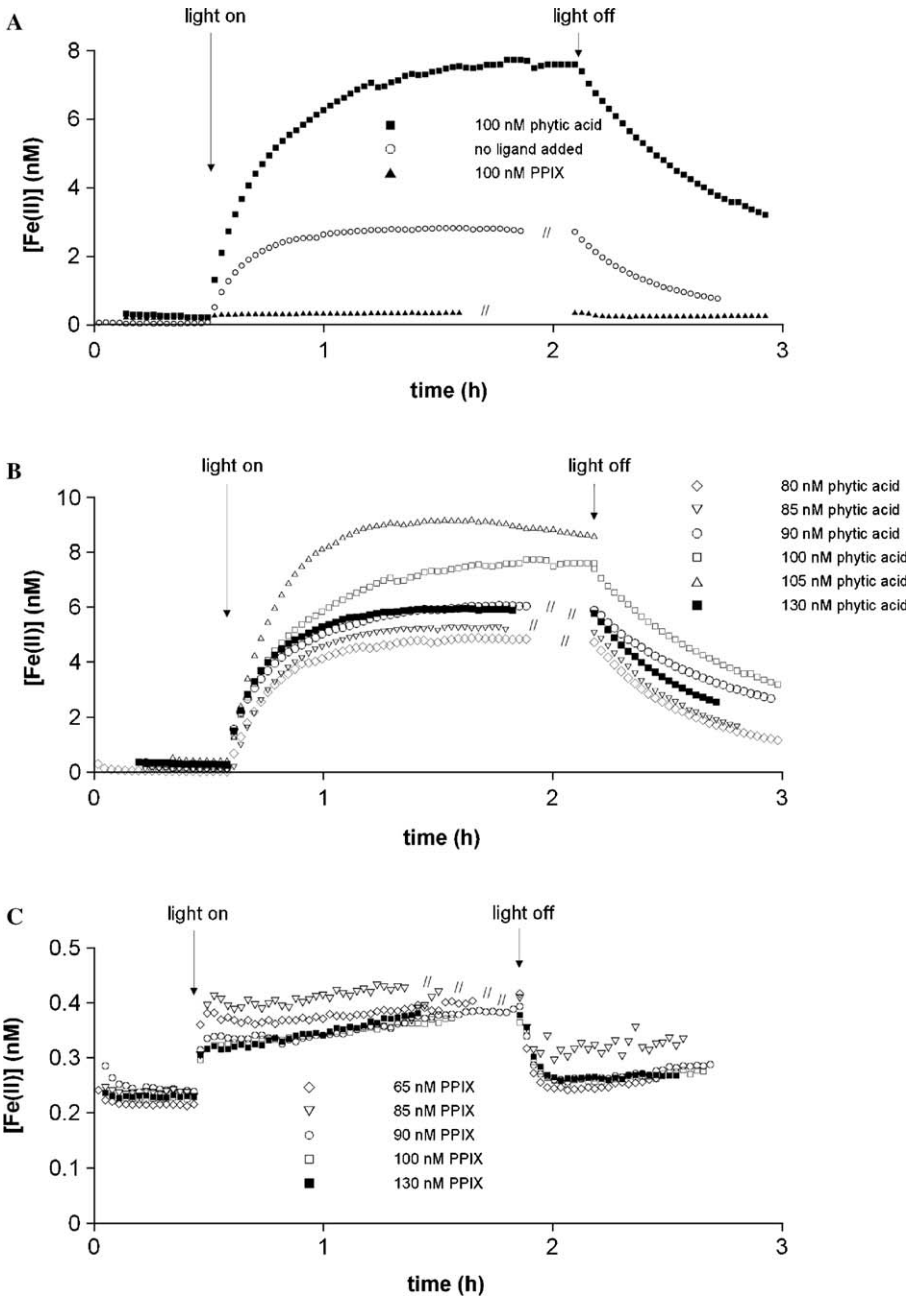

Fig. 7. (A) The photoproduction of Fe(II) after a 100 nM Fe(III) addition to seawater containing no added ligands (control) in comparison with the addition of 100 nM phytic acid and 100 nM PPIX. (B) The photoproduction of Fe(II) with increasing concentrations phytic acid (80, 85, 90, 100, 105, and 130 nM phytic acid). (C) The photoproduction of Fe(II) with increasing concentrations PPIX (65, 85, 90, 100, and 130 nM PPIX).

not totally dissolve at higher concentrations. Nevertheless, because the effect of PPIX addition on the photoproduction of Fe(II) was demonstrated to be large (Figs. 7A and C), and this could not be explained by the binding of Fe(III) by PPIX, we investigated the possible role of PPIX in binding Fe(II).

A series of experiments was performed where we compared the decrease in the concentration of Fe(II) due to the addition of different concentrations of PPIX Eq. (3) with the disappearance of Fe(II) by oxidation alone Eq. (6) (Fig. 10). Reactions with Fe(II) in seawater containing PPIX can be described by the binding of Fe(II) by PPIX:

$$[\mathrm{Fe(II)}] + [\mathrm{PPIX}] \xrightarrow{k_{\mathrm{Fe(II)PPIX}}} [\mathrm{Fe(II)PPIX}] \quad (1)$$

and the parallel (hence competing) oxidation reaction of Fe(II),

$$[\mathrm{Fe(II)}] \xrightarrow{k_{\mathrm{ox}}} [\mathrm{Fe(III)}] \quad (2)$$

We assumed that no reduction of Fe(III) could take place during our experiments and that the dissociation of the Fe(II)PPIX complex is much slower then the reverse association of Fe(II) to PPIX. Pseudo first order kinetics was assumed for oxidation as well as the combination of oxidation and binding of Fe(II) by PPIX (excess of PPIX

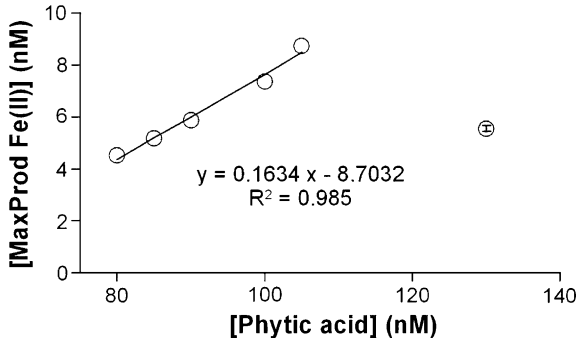

Fig. 8. The concentration of MaxProd Fe(II) upon addition of increasing concentrations phytic acid and 100 nM Fe(III) to seawater. The photochemical experiment with 130 nM DFOB was performed twice.

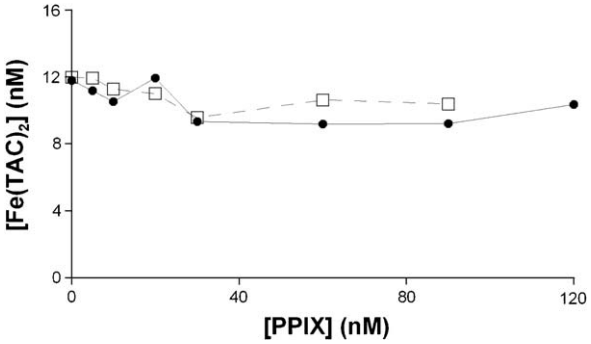

Fig. 9. TAC-labile Fe(III) (the concentration $Fe(TAC)_2$ after 12 h equilibration) versus increasing concentrations of PPIX. Increasing concentrations of PPIX do not result in decreasing TAC-labile Fe(III) which indicates that PPIX does not bind Fe(III) under the prevailing conditions. The experiment was performed twice.

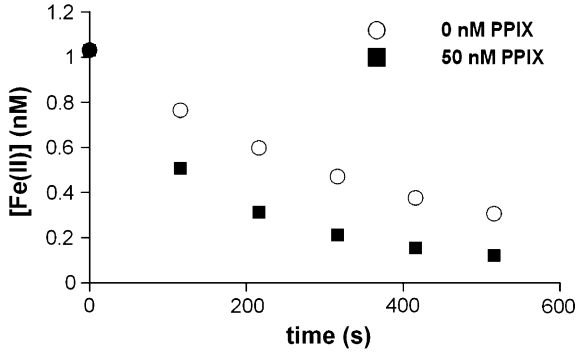

Fig. 10. (A) The concentration of Fe(II) (1 nM Fe(II)) decreasing with time due to oxidation without the addition of PPIX and due to the combination of oxidation and binding by PPIX (1 nM Fe(II) and 50 nM PPIX added).

and oxidants). Integration (assuming that $[Fe(II)] = [Fe(II)_0]$ at $t = 0$) of the differential equations for the reactions with Fe(II) in seawater containing PPIX:

$$\frac{d[Fe(II)]}{dt} = -k_{Fe(II)PPIX} \cdot [Fe(II)] \cdot [PPIX] - k_{ox} \cdot [Fe(II)], \quad (3)$$

$$\frac{d[Fe(II)]}{dt} = -\left(k_{Fe(II)PPIX} \cdot [PPIX] + k_{ox}\right) \cdot [Fe(II)], \quad (4)$$

$$\frac{d[Fe(II)]}{dt} = -(k_{overall}) \cdot [Fe(II)], \quad (5)$$

and for seawater without PPIX:

$$\frac{d[Fe(II)]}{dt} = -k_{ox} \cdot [Fe(II)] \quad (6)$$

resulted in a linear relationship between the natural logarithm of the concentration Fe(II) with time.

The rate constant for the binding of Fe(II) by PPIX ($k_{Fe(II)PPIX}$ [PPIX]) depends on the PPIX concentration and was calculated by subtracting the rate constant of the oxidation of Fe(II) without PPIX from the rate constant for the combination of oxidation and binding in the presence of PPIX (5),

$$k_{Fe(II)PPIX} \cdot [PPIX] = k_{overall} - k_{ox}. \quad (7)$$

The $k_{Fe(II)PPIX}$ [PPIX] was calculated for PPIX concentrations between 25 and 100 nM Eq. (7) (Fig. 11) and varied between of $3.0 \times 10^{-3} \pm 9.7 \times 10^{-4}\ s^{-1}$ ($n = 2$) for 25 nM PPIX, $4.5 \times 10^{-3} \pm 9.8 \times 10^{-4}\ s^{-1}$ ($n = 4$) for 50 nM PPIX, and $1.02 \times 10^{-2} \pm 7.9 \times 10^{-4}\ s^{-1}$ ($n = 2$) for 100 nM PPIX. These values may be underestimated as the Fe(II) oxidation rate appeared to decrease independent of irradiance time with increasing concentration PPIX in our photochemical experiments. In spite of the questions raised about the solubility of PPIX a positive linear relationship between the $k_{Fe(II)PPIX}$ and the concentration PPIX was found, with a slope of $1.0 \times 10^{-4}\ nM^{-1}$ PPIX. In other words the rate constant normalized to 1 nM PPIX is: $k_{Fe(II)PPIX} = (k_{overall} - k_{ox})/[PPIX] = 1.04 \times 10^{-4} \pm 1.53 \times 10^{-5}\ s^{-1}\ nM^{-1}$ PPIX.

Apparently PPIX in seawater hardly binds Fe(III) but Fe(II) instead. An addition of PPIX concentrations between 65 and 130 nM is thus always in excess of 2.81 nM Fe(II) (as formed in the control, 100 nM Fe(III), no ligands), which explains why we did not see any effects on the photochemical characteristics by increasing concentrations of PPIX.

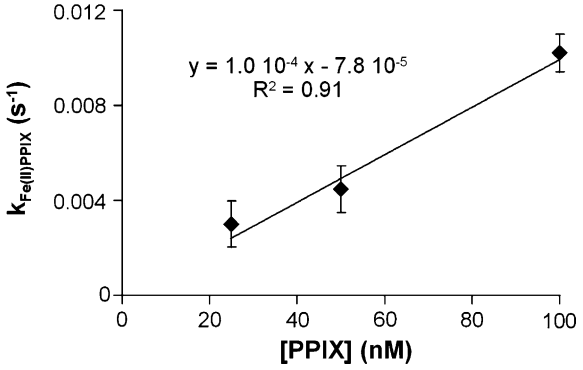

Fig. 11. The obtained rate constant of the binding of Fe(II) by PPIX ($k_{Fe(II)PPIX}$) versus the total concentration of added PPIX. Shown are the averaged values and their standard errors: the trend line is based on all the individual data, the slope is significant ($P < 0.001$).

Upon turning off the light, the Fe(II) concentration decreased quickly to a minimum due to oxidation but then, interestingly, the Fe(II) concentration increased again. In contrast to the photochemical experiments with other organic Fe-binding ligands, the experiments with PPIX showed a process of Fe(III) reduction proceeding after the light was switched off (Fig. 12). A distinct linear relationship was found plotting the Fe(II) production rate (nM/h) in the dark versus the duration of the irradiance treatment (Fig. 13). The Fe(II) production rate in the dark increased with 0.10 nM h^{-1} for each hour of preceding irradiance during the experiments ($R^2 = 0.99$) (Fig. 13). Dark reduction of Fe(III) is often assigned to reduction of Fe(III) by photoproduced superoxide (Voelker and Sedlak, 1995; Emmenegger et al., 2001; Croot et al., 2005) or free radical organic ligand species (Faust, 1994).

A hint suggesting that superoxide might play a role in the reduction of Fe(III) in the dark was given by the concentration of H_2O_2 produced during irradiation of seawater containing Fe(III) and PPIX. Photochemical experiments (each with 100 nM Fe(III)) with 100 nM DFOB produced 2.85 nM H_2O_2 h^{-1}, with 100 nM phytic acid produced 1.53 nM H_2O_2 h^{-1} and 80 nM PPIX produced 6.85 nM H_2O_2 h^{-1}. The concentrations H_2O_2 produced during the experiments in the presence of PPIX are 2.5–4.5 times higher than with DFOB or phytic acid. Bimolecular dismutation of superoxide is postulated as the main source of hydrogen peroxide in the open ocean (Petasne and Zika, 1987). The fast oxidation of Fe(II) by superoxide also produces hydrogen peroxide (Weis, 1935), however, the reduction reaction of superoxide with trace metals is faster then the oxidation reaction in seawater (Voelker and Sedlak, 1995).

Although speculative for water and seawater, it has been shown that iron porphyrins show catalytic behavior, efficiently catalyzing thermal redox reactions on organic substrates by reversible modification of the oxidation state of the metal center (Suslick and Watson, 1992; Maldotti et al., 1993; Frausto da Silva and Williams, 1994). The irradiation of iron porphyrin complexes could via an axial ligand to metal charge transfer (LMCT) realize a photo-assisted redox cycle in which molecular oxygen is activated by coordination to Fe(II) in the ferrous porphyrin complex leading to the production of superoxide and radical ligand species (Maldotti et al., 1989). The Fe(II)PPIX oxidation reaction could form a source for the production of superoxide in the dark and explain our results on Fe(II) production in the dark. Further testing is needed to prove that a similar catalytic photosensitizing redox cycling could occur with FePPIX in seawater.

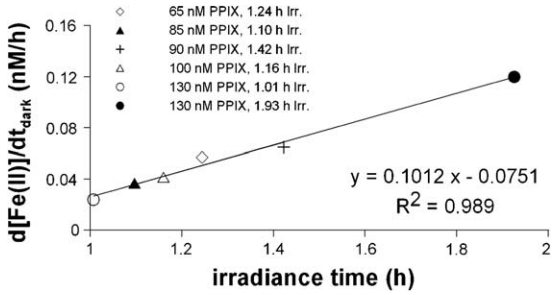

Fig. 13. The Fe(II) production rate in the dark after irradiance, versus the irradiance time for seawater containing 100 nM Fe(III) and various concentrations PPIX (though all in excess over Fe(II)).

4. Conclusion

Freshly formed amorphous Fe(III) hydroxides were the main source for the photoproduction of Fe(II). As a consequence, the organic Fe-binding ligands affecting the concentration of amorphous Fe(III) hydroxides will have an effect on the photoproduced Fe(II) concentration. Yet, our experiments with PPIX show that there are also other modes of interactions decreasing the concentration of photoproduced Fe(II).

This study shows that the photochemistry of Fe(III) can be strongly affected by the presence of organic Fe-binding ligands. The identity of the organic Fe-binding ligand and subsequently its interaction with the Fe(III) or Fe(II) determines the final photoproduced Fe(II) concentration.

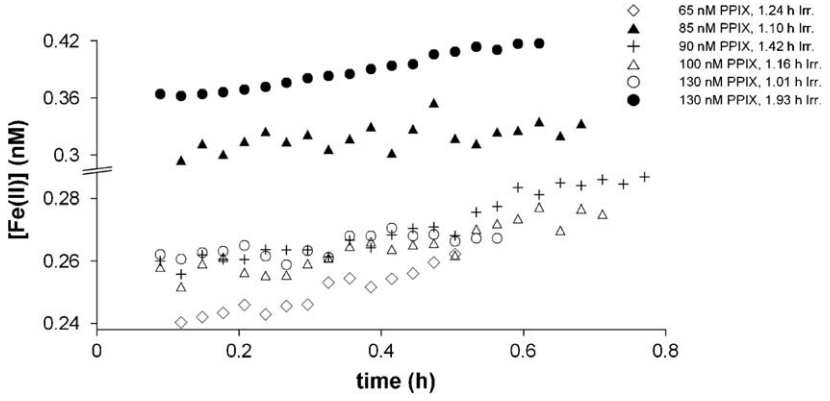

Fig. 12. The increase in the concentration Fe(II) in the dark in seawater containing increasing concentrations of PPIX and varying irradiation duration (h Irr.) between 1 and 2 h. This figure contains the same data as Fig. 7C with the added results from a second experiment with 130 nM PPIX (closed circles) (Table 2).

Phaeophytin, as well as phytic acid showed a higher MaxProd Fe(II) compared to ferrichrome and the control without added ligands. A more detailed study with phytic acid suggested that the increase in the photoreducible Fe(III) fraction results from the more loosely aggregation of Fe(III) as a consequence of co-aggregation with phytic acid. The excess phytic acid not co-aggregated with the Fe(III) is suggested to bind surface Fe(III) and shield it from photoreduction. The PPIX binds Fe(II) reducing the free photoproduced Fe(II) concentration. Furthermore, a dark production of Fe(II) related to the preceding irradiance time of the experiments is suggestive of a process where oxidation of Fe(II) PPIX leads to the production of superoxide, as has been reported previously for Fe-porphyrin complexes in oxygenated aqueous ethanol (Maldotti et al., 1989).

As the photo-induced redox cycle is important in the creation of biological available Fe (Wells and Mayer, 1991; Johnson et al., 1994; Miller and Kester, 1994a) the investigation of the influence of organic complexation on the photoreduction of Fe(III) is crucial. This is especially true, because it has been reported that 99% of the dissolved Fe concentration in the oceans is organically complexed (Gledhill and van den Berg, 1994). Our knowledge of organic Fe complexation in the oceanic environment is limited, thus in order to fully understand the role of organic Fe-binding ligands in the seawater Fe photochemistry it is necessary to identify and quantify organic Fe-binding ligands.

Although the presence of DFOB, PPIX, and phytic acid in the marine environment is shown, their presence can not yet be quantified. This makes an evaluation of the ecological consequences difficult. Nevertheless, in marine environments where the phytoplankton community is dependent on rapid Fe recycling of a very small Fe pool (Cullen et al., 1992; Price et al., 1994) much of the regenerated iron might be present in biological chelates such as porphyrin related molecules, whose release into seawater could have an important influence on the redox speciation of Fe. Furthermore, phytic acid makes up an important part of the phosphate entering the sea via rivers and could play an important role in the photochemistry of Fe(III) in coastal waters (Suzumura and Kamatani, 1995). It is shown that the phytic acid Fe complex provides biological available Fe for phytoplankton (Maldonado et al., 2005). These results show that it is important to take the Fe(III) photochemistry in consideration when investigating the bioavailability of Fe(III) complexed by any given organic Fe-binding ligand in culture experiments.

Acknowledgments

We want to thank Anita Buma (RuG), Patrick Laan (Royal NIOZ), Klaas Timmermans (Royal NIOZ), Bert Wolterbeek (IRI, University of Delft), and Lisa Weber (NOC, Southampton) for their help and advice. Ebel Top (RuG) is appreciated for the construction of the PMMA bottles. Vicky Carolus of the Hogeschool Drenthe, Emmen (Netherlands), Ilona Velzeboer of the Fontys Hogescholen, Eindhoven (Netherlands), and Justin Swart of the Hogeschool van Utrecht (Netherlands) performed much of the measurements during their traineeship at Royal NIOZ. Furthermore, we want to thank the three anonymous reviewers for their helpful comments. This research is funded by NWO/NAAP Grant No. 85120004.

Associate editor: Robert H. Byrne

References

Anderson, G., 1963. Effect of iron/phosphorus ratio and acid concentration on precipitation of ferric inositol hexaphosphate. *J. Sci. Food Agric.* **14**, 352–359.

Anderson, M.A., Morel, F.M.M., 1980. Uptake of Fe(II) by a diatom in oxic culture medium. *Mar. Biol. Lett.* **1**, 263–268.

Anderson, M.A., Morel, F.M.M., 1982. The influence of aqueous iron chemistry on the uptake of iron by the coastal diatom Thalassiosira weissflogii. *Limnol. Oceanogr.* **27**, 789–813.

Barbeau, K., Rue, E.L., Bruland, K.W., Butler, A., 2001. Photochemical cycling of iron in the surface ocean mediated by microbial iron(III)-binding ligands. *Nature* **413**, 409–413.

Barbeau, K., Rue, E.L., Trick, C.G., Bruland, K.T., Butler, A., 2003. Photochemical reactivity of siderophores produced by marine heterotrophic bacteria and cyanobacteria based on characteristic Fe(III) binding groups. *Limnol. Oceanogr.* **48**, 1069–1078.

Bowie, A.R., Achterberg, E.P., Croot, P.L., de Baar, H.J.W., Laan, P., Moffett, J.W., Ussher, S., Worsfold, P.J., 2006. A community-wide intercomparison exercise for the determination of dissolved iron in seawater. *Mar. Chem.* **98**, 81–99.

Bowie, A.R., Achterberg, E.P., Sedwick, P.N., Ussher, S., Worsfold, P.J., 2002. Real-time monitoring of picomolar concentrations of iron(II) in marine waters using automated flow injection-chemiluminescence instrumentation. *Environ. Sci. Technol.* **36**, 4600–4607.

Boyé, M., Aldrich, A.P., van den Berg, C.M.G., de Jong, J.T.M., Veldhuis, M., de Baar, H.J.W., 2003. Horizontal gradient of the chemical speciation of iron in surface waters of the northeast Atlantic Ocean. *Mar. Chem.* **80**, 129–143.

Boyé, M., Nishioka, J., Croot, P.L., Laan, P., Timmermans, K.R., de Baar, H.J.W., 2005. Major deviations of iron complexation during 22 days of a mesoscale iron enrichment in the open Southern Ocean. *Mar. Chem.* **96**, 257–271.

Boyé, M., van den Berg, C.M.G., de Jong, J.T.M., Leach, H., Croot, P.L., de Baar, H.J.W., 2001. Organic complexation of iron in the Southern Ocean. *Deep Sea Res. I* **48**, 1477–1497.

Bruland, K.W., Rue, E.L., Smith, G.J., 2001. Iron and macronutrients in California coastal upwelling regimes: implications for diatom blooms. *Limnol. Oceanogr.* **46**, 1661–1674.

Celi, L., De Luca, G., Barberis, E., 2003. Effects of interaction of organic and inorganic P with ferrihydrite and kaolinite-iron oxide systems on iron release. *Soil Sci.* **168**, 479–488.

Cornell, R.M., Schwertmann, U., 1996. *The Iron Oxides*. VCH Publishers.

Croot, P.L., Bowie, A.R., Frew, R.D., Maldonado, M.T., Hall, J.A., Safi, K.A., la Roche, J., Boyd, P.W., Law, C.S., 2001. Retention of dissolved iron and Fe-II in an iron induced Southern Ocean phytoplankton bloom. *Geophys. Res. Lett.* **28**, 3425–3428.

Croot, P.L., Johansson, M., 2000. Determination of iron speciation by cathodic stripping voltammetry in seawater using the competing ligand 2-(2- thiazolylazo)-*p*-cresol (TAC). *Electroanalysis* **12**, 565–576.

Croot, P.L., Laan, P., Nishioka, J., Strass, V., Cisewski, B., Boye, M., Timmermans, K.R., Bellerby, R.G., Goldson, L., Nightingale, P., de Baar, H.J.W., 2005. Spatial and temporal distribution of Fe(II) and H2O2 during EisenEx, an open ocean mesoscale iron enrichment. *Mar. Chem.* **95**, 65–88.

Cullen, J.J., Lewis, M.R., Davis, C.O., Barber, R.T., 1992. Photosynthetic characteristics and estimated growth-rates indicate grazing is the proximate control of primary production in the equatorial Pacific. *J. Geophys. Res.* **97**, 639–654.

de Baar, H.J.W., Boyd, P.W., 2000. The role of iron in plankton ecology and carbon dioxide transfer of the global oceans. In: Hanson, R.B., Ducklow, H.W., Field, J.G. (Eds.), *The Dynamic Ocean Carbon Cycle; A Midterm Synthesis of the Joint Global Ocean Flux Study*, vol. 61–140. Cambridge University Press, Cambridge, MA.

de Baar, H.J.W., Boyd, P.W., Coale, K.H., Landry, M.R., Tsuda, A., Assmy, P., Bakker, D.C.E., Bozec, Y., Barber, R.T., Brzezinski, M.A., Buesseler, K.O., Boye, M., Croot, P.L., Gervais, F., Gorbunov, M.Y., Harrison, P.J., Hiscock, W.T., Laan, P., Lancelot, C., Law, C.S., Levasseur, M., Marchetti, A., Millero, F.J., Nishioka, J., Nojiri, Y., van Oijen, T., Riebesell, U., Rijkenberg, M.J.A., Saito, H., Takeda, S., Timmermans, K.R., Veldhuis, M.J.W., Waite, A.M., Wong, C.S., 2005. Synthesis of iron fertilization experiments: From the iron age in the age of enlightenment. *J. Geophys. Res.* **110**, C09S16. doi:10.1029/2004JC002601.

de Baar, H.J.W., Buma, A.G.J., Nolting, R.F., Cadee, G.C., Jacques, G., Treguer, P.J., 1990. On iron limitation of the Southern Ocean—experimental—observations in the Weddell and Scotia seas. *Mar. Ecol. Progr. Ser.* **65**, 105–122.

de Jong, J.T.M., den Das, J., Bathmann, U., Stoll, M.H.C., Kattner, G., Nolting, R.F., de Baar, H.J.W., 1998. Dissolved iron at subnanomolar levels in the Southern Ocean as determined by ship-board analysis. *Anal. Chim. Acta* **377**, 113–124.

Emmenegger, L., Schonenberger, R.R., Sigg, L., Sulzberger, B., 2001. Light-induced redox cycling of iron in circumneutral lakes. *Limnol. Oceanogr.* **46**, 49–61.

Faust, B.C., 1994. A review of the photochemical redox reactions of iron(III) species in atmospheric, oceanic, and surface waters: influences on geochemical cycles and oxidant formation. In: Helz, G.R., Zepp, R.G., Crosby, D.G. (Eds.), *Aquatic Surface Photochemistry*. CRC Press, Inc., Boca Raton, FL, pp. 3–37.

Frausto da Silva, J.J.R., Williams, R.J.P., 1994. Haem iron: coupled redox reactions. In: *The Biological Chemistry of the Elements*. Clarendon Press, Oxford, pp. 343–369.

Geider, R.J., la Roche, J., 1994. The role of iron in phytoplankton photosynthesis, and the potential for iron-limitation of primary productivity in the sea. *Photosynth. Res.* **39**, 275–301.

Geider, R.J., la Roche, J., Greene, R.M., Olaizola, M., 1993. Response of the photosynthetic apparatus of *Phaeodactylum tricornutum*, Bacillariophyceae. to nitrate, phosphate, or iron starvation. *J. Phycol.* **29**, 755–766.

Gerringa, L.J.A., de Baar, H.J.W., Timmermans, K.R., 2000. A comparison of iron limitation of phytoplankton in natural oceanic waters and laboratory media conditioned with EDTA. *Mar. Chem.* **68**, 335–346.

Gerringa, L.J.A., Rijkenberg, M.J.A., Timmermans, K.R., Buma, A.G.J., 2004. The influence of solar ultraviolet radiation on the photochemical production of H_2O_2 in the equatorial Atlantic Ocean. *J. Sea Res.* **51**, 3–10.

Gledhill, M., McCormack, P., Ussher, S., Achterberg, E.P., Mantoura, R.F.C., Worsfold, P.J., 2004. Production of siderophore type chelates by mixed bacterioplankton populations in nutrient enriched seawater incubations. *Mar. Chem.* **88**, 75–83.

Gledhill, M., van den Berg, C.M.G., 1994. Determination of complexation of iron(III) with natural organic complexing ligands in seawater using cathodic stripping voltammetry. *Mar. Chem.* **47**, 41–54.

Gledhill, M., van den Berg, C.M.G., Nolting, R.F., Timmermans, K.R., 1998. Variability in the speciation of iron in the northern North Sea. *Mar. Chem.* **59**, 283–300.

Granger, J., Price, N.M., 1999. The importance of siderophores in iron nutrition of heterotrophic marine bacteria. *Limnol. Oceanogr.* **44**, 541–555.

Greene, R.M., Geider, R.J., Falkowski, P.G., 1991. Effect of iron limitation on photosynthesis in a marine diatom. *Limnol. Oceanogr.* **36**, 1772–1782.

Harrison, G.I., Morel, F.M.M., 1986. Response of the marine diatom *Thalassiosira weisflogii* to iron stress. *Limnol. Oceanogr.* **31**, 989–997.

Hudson, R.J.M., Covault, D.T., Morel, F.M.M., 1992. Investigations of iron coordination and redox reactions in seawater using Fe-59 radiometry and ion-pair solvent-extraction of amphiphilic iron complexes. *Mar. Chem.* **38**, 209–235.

Hutchins, D.A., Bruland, K.W., 1998. Iron-limited diatom growth and Si:N uptake ratios in a coastal upwelling regime. *Nature* **393**, 561–564.

Johnson, K.S., Coale, K.H., Elrod, V.A., Tindale, N.W., 1994. Iron photochemistry in seawater from the equatorial Pacific. *Mar. Chem.* **46**, 319–334.

Johnson, K.S., Gordon, R.M., Coale, K.H., 1997. What controls dissolved iron concentrations in the world ocean? *Mar. Chem.* **57**, 137–161.

King, D.W., Lounsbury, H.A., Millero, F.J., 1995. Rates and mechanism of Fe(II) oxidation at nanomolar total iron concentrations. *Environ. Sci. Technol.* **29**, 818–824.

Kuma, K., Nakabayashi, S., Matsunaga, K., 1995. Photoreduction of Fe(III) by hydroxycarboxylic acids in seawater. *Water Res.* **29**, 1559–1569.

Kuma, K., Nishioka, J., Matsunaga, K., 1996. Controls on iron(III) hydroxide solubility in seawater: the influence of pH and natural organic chelators. *Limnol. Oceanogr.* **41**, 396–407.

Kunkely, H., Vogler, A., 2001. Photoreduction of aqueous ferrioxamine B by oxalate induced by outer-sphere charge transfer excitation. *Inorg. Chem. Commun.* **4**, 215–217.

Liu, X.W., Millero, F.J., 1999. The solubility of iron hydroxide in sodium chloride solutions. *Geochim. Cosmochim. Acta* **63**, 3487–3497.

Liu, X.W., Millero, F.J., 2002. The solubility of iron in seawater. *Mar. Chem.* **77**, 43–54.

Macrellis, H.M., Trick, C.G., Rue, E.L., Smith, G., Bruland, K.W., 2001. Collection and detection of natural iron-binding ligands from seawater. *Mar. Chem.* **76**, 175–187.

Maldonado, M.T., Price, N.M., 2000. Nitrate regulation of Fe reduction and transport by Fe-limited *Thalassiosira oceanica*. *Limnol. Oceanogr.* **45**, 814–826.

Maldonado, M.T., Price, N.M., 2001. Reduction and transport of organically bound iron by *Thalassiosira oceanica* (Bacillariophyceae). *J. Phycol.* **37**, 298–309.

Maldonado, M.T., Strzepek, R.F., Sander, S., Boyd, P.W., 2005. Acquisition of iron bound to strong organic complexes, with different Fe-binding groups and photochemical reactivities, by plankton communities in Fe-limited subantarctic waters. *Glob. Biogeochem. Cycl.* **19**, GB4S23, doi:doi:10.1029/2005GB002481.

Maldotti, A., Amadelli, R., Bartocci, C., Carassiti, V., Polo, E., Varani, G., 1993. Photochemistry of iron-porphyrin complexes—biomimetics and catalysis. *Coord. Chem. Rev.* **125**, 143–154.

Maldotti, A., Bartocci, C., Amadelli, R., Carassiti, V., 1989. Photocatalytic reactions in the 2,3,7,8,12,13,17,18-octaethyl-porphyrinato-iron(III) ethanol carbon-tetrachloride system. *J. Chem. Soc., Dalton Trans.*, 1197–1201.

Martin, J.H., Fitzwater, S.E., 1988. Iron-deficiency limits phytoplankton growth in the northeast Pacific subarctic. *Nature* **331**, 341–343.

Martinez, J.S., Haygood, M.G., Butler, A., 2001. Identification of a natural desferrioxamine siderophore produced by a marine bacterium. *Limnol. Oceanogr.* **46**, 420–424.

McCormack, P., Worsfold, P.J., Gledhill, M., 2003. Separation and detection of siderophores produced by marine bacterioplankton using high-performance liquid chromatography with electrospray ionization mass spectrometry. *Anal. Chem.* **75**, 2647–2652.

Miller, W.L., Kester, D., 1994a. Photochemical iron reduction and iron bioavailability in seawater. *J. Mar. Res.* **52**, 325–343.

Miller, W.L., Kester, D.R., 1988. Hydrogen peroxide measurement in seawater by (para- hydroxyphenyl)acetic acid dimerization. *Anal. Chem.* **60**, 2711–2715.

Miller, W.L., Kester, D.R., 1994b. Peroxide variations in the Sargasso sea. *Mar. Chem.* **48**, 17–29.

Millero, F.J., 1998. Solubility of Fe(III) in seawater. *Earth Planet Sci. Lett.* **154**, 323–329.

Millero, F.J., Sotolongo, S., 1989. The oxidation of Fe(II) with H_2O_2 in seawater. *Geochim. Cosmochim. Acta* **53**, 1867–1873.

Millero, F.J., Sotolongo, S., Izaguirre, M., 1987. The oxidation-kinetics of Fe(II) in seawater. *Geochim. Cosmochim. Acta* **51**, 793–801.

Moffett, J.W., 2001. Transformations among different forms of iron in the ocean. In: Turner, D.R., Hunter, K.A. (Eds.), *The Biogeochemistry of Iron in Seawater*, vol. 7. John Wiley & Sons, New York, pp. 343–372.

Nishioka, J., Takeda, S., de Baar, H.J.W., Croot, P.L., Boye, M., Laan, P., Timmermans, K.R., 2005. Changes in the concentration of iron in different size fractions during an iron enrichment experiment in the open Southern Ocean. *Mar. Chem.* **95**, 51–63.

Nolting, R.F., Gerringa, L.J.A., Swagerman, M.J.W., Timmermans, K.R., de Baar, H.J.W., 1998. Fe(III) speciation in the high nutrient, low chlorophyll Pacific region of the Southern Ocean. *Mar. Chem.* **62**, 335–352.

Ognalaga, M., Frossard, E., Thomas, F., 1994. Glucose-1-phosphate and myoinositol hexaphosphate adsorption mechanisms on goethite. *Soil Sci. Soc. Am. J.* **58**, 332–337.

Parfitt, R.L., 1989. Phosphate reactions with natural allophane, ferrihydrite and goethite. *J. Soil Sci.* **40**, 359–369.

Pehkonen, S.O., Siefert, R., Erel, Y., Webb, S., Hoffmann, M.R., 1993. Photoreduction of iron oxyhydroxides in the presence of important atmospheric organic-compounds. *Environ. Sci. Technol.* **27**, 2056–2062.

Pehkonen, S.O., Siefert, R.L., Hoffmann, M.R., 1995. Photoreduction of iron oxyhydroxides and the photooxidation of halogenated acetic-acids. *Environ. Sci. Technol.* **29**, 1215–1222.

Petasne, R.G., Zika, R.G., 1987. Fate of superoxide in coastal seawater. *Nature* **325**, 516–518.

Price, N.M., Ahner, B.A., Morel, F.M.M., 1994. The equatorial Pacific Ocean—grazer-controlled phytoplankton populations in an iron-limited ecosystem. *Limnol. Oceanogr.* **39**, 520–534.

Pullin, M.J., Cabaniss, S.E., 2003. The effects of pH, ionic strength, and iron-fulvic acid interactions on the kinetics of non-photochemical iron transformations. II. The kinetics of thermal reduction. *Geochim. Cosmochim. Acta* **67**, 4079–4089.

Raven, J.A., 1990. Predictions of Mn and Fe use efficiencies of phototrophic growth as a function of light availability for growth and of C assimilation pathway. *New Phytologist* **116**, 1–18.

Rijkenberg, M.J.A., Fischer, A.C., Kroon, J.J., Gerringa, L.J.A., Timmermans, K.R., Wolterbeek, H.T., de Baar, H.J.W., 2005. The influence of UV irradiation on the photoreduction of iron in the Southern Ocean. *Mar. Chem.* **93**, 119–129.

Rijkenberg, M.J.A., Gerringa, L.J.A., Neale, P.J., Timmermans, K.R., Buma, A.G.J., de Baar, H.J.W., 2004. UVA variability overrules UVB ozone depletion effects on the photoreduction of iron in the Southern Ocean. *Geophys. Res. Lett.*, 31.

Rose, A.L., Waite, T.D., 2002. Kinetic model for Fe(II) oxidation in seawater in the absence and presence of natural organic matter. *Environ. Sci. Technol.* **36**, 433–444.

Rue, E.L., Bruland, K.W., 1995. Complexation of iron(III) by natural organic-ligands in the central north Pacific as determined by a new competitive ligand equilibration adsorptive cathodic stripping voltammetric method. *Mar. Chem.* **50**, 117–138.

Rue, E.L., Bruland, K.W., 1997. The role of organic complexation on ambient iron chemistry in the equatorial Pacific Ocean and the response of a mesoscale iron addition experiment. *Limnol. Oceanogr.* **42**, 901–910.

Rueter, J.G., Ades, D.R., 1987. The role of iron nutrition in photosynthesis and nitrogen assimilation in *Scenedesmus quadricauda* (Chlorophyceae). *J. Phycol.* **23**, 452–457.

Rueter, J.G., Ohki, K., Fujita, Y., 1990. The effect of iron nutrition on photosynthesis and nitrogen-fixation in cultures of *Trichodesmium* (Cyanophyceae). *J. Phycol.* **26**, 30–35.

Santana-Casiano, J.M., Gonzalez-Davila, M., Millero, F.J., 2004. The oxidation of Fe(II) in NaCl-HCO_3- and seawater solutions in the presence of phthalate and salicylate ions: a kinetic model. *Mar. Chem.* **85**, 27–40.

Santana-Casiano, J.M., Gonzalez-Davila, M., Rodriguez, M.J., Millero, F.J., 2000. The effect of organic compounds in the oxidation kinetics of Fe(II). *Mar. Chem.* **70**, 211–222.

Schwertmann, U., Fischer, W.R., 1973. Natural amorphous ferric hydroxide. *Geoderma* **10**, 237–247.

Schwertmann, U., Taylor, R.M., 1972. The transformationof lepidocrocite to goethite. *Clays Clay Miner.* **20**, 151–158.

Schwertmann, U., Thalmann, H., 1976. The influence of [FeII], [Si], and pH on the formation of lepidocrocite and ferrihydrite during oxidation of aqueous $FeCl_2$ solutions. *Clay Miner.* **11**, 189–200.

Siffert, C., Sulzberger, B., 1991. Light-induced dissolution of hematite in the presence of oxalate—a case-study. *Langmuir* **7**, 1627–1634.

Steeneken, S.F., Buma, A.G.J., Gieskes, W.W.C., 1995. Changes in transmission characteristics of polymethylmethacrylate and cellulose-(III) acetate during exposure to ultraviolet-light. *Photochem. Photobiol.* **61**, 276–280.

Strzepek, R.F., Harrison, P.J., 2004. Photosynthetic architecture differs in coastal and oceanic diatoms. *Nature* **431**, 689–692.

Sulzberger, B., Laubscher, H., 1995. Photochemical reductive dissolution of lepidocrocite—effect of pH. *Aquat. Chem. Adv. Chem. Ser.* **244**, 279–290.

Suslick, K.S., Watson, R.A., 1992. The photochemistry of chromium, manganese, and iron porphyrin complexes. *New J. Chem.* **16**, 633–642.

Suzumura, M., Kamatani, A., 1995. Origin and distribution of inositol hexaphosphate in estuarine and coastal sediments. *Limnol. Oceanogr.* **40**, 1254–1261.

Takeda, S., Kamatani, A., 1989. Photoreduction of Fe(III)-EDTA complex and its availability to the coastal diatom *Thalassiosira weissflogii. Red Tides: Biol. Environ. Sci. Toxicol.*, 349–352.

Theis, T.L., Singer, P.C., 1974. Complexation of iron(II) by organic matter and its effect on iron(II) oxygenation. *Environ. Sci. Technol.* **8**, 569–573.

Tipping, E., Thompson, D.W., Woof, C., 1989. Iron-oxide particulates formed by the oxygenation of natural and model lakewaters containing Fe(II). *Archiv Fur Hydrobiologie* **115**, 59–70.

Trick, C.G., 1989. Hydroxamate-siderophore production and utilization by marine eubacteria. *Curr. Microbiol.* **18**, 375–378.

van den Berg, C.M.G., 1995. Evidence for organic complexation of iron in seawater. *Mar. Chem.* **50**, 139–157.

Voelker, B.M., Morel, F.M.M., Sulzberger, B., 1997. Iron redox cycling in surface waters: effects of humic substances and light. *Environ. Sci. Technol.* **31**, 1004–1011.

Voelker, B.M., Sedlak, D.L., 1995. Iron reduction by photoproduced superoxide in seawater. *Mar. Chem.* **50**, 93–102.

Waite, T.D., 2001. Thermodynamics of the iron system in seawater. In: Turner, D.R., Hunter, K.A. (Eds.), *The Biogeochemistry of Iron in Seawater*, vol. 7. John Wiley & Sons, New York, pp. 291–342.

Waite, T.D., Morel, F.M.M., 1984. Photoreductive dissolution of colloidal iron-oxide—effect of citrate. *J. Colloid Interface Sci.* **102**, 121–137.

Waite, T.D., Torikov, A., 1987. Photo-assisted dissolution of colloidal iron-oxides by thiol- containing compounds 2. Comparison of lepidocrocite (gamma- FeOOH) and hematite (alpha-Fe_2O_3) dissolution. *J. Colloid Interface Sci.* **119**, 228–235.

Waite, T.D., Torikov, A., Smith, J.D., 1986. Photoassisted dissolution of colloidal iron-oxides by thiol- containing compounds 1. Dissolution of hematite (alpha-Fe_2O_3). *J. Colloid Interface Sci.* **112**, 412–420.

Weis, J., 1935. Elektronenübergangsprozesse im Mechanismus von Oxidations- und reduktionsreaktionen in Lösungen. *Die Naturwissenschaften* **4**, 64–69.

Wells, M.L., Mayer, L.M., 1991. The photoconversion of colloidal iron oxyhydroxides in seawater. *Deep Sea Res. I* **38**, 1379–1395.

Wells, M.L., Trick, C.G., 2004. Controlling iron availability to phytoplankton in iron-replete coastal waters. *Mar. Chem.* **86**, 1–13.

Wilhelm, S.W., Trick, C.G., 1994. Iron-limited growth of cyanobacteria: multiple siderophore production is a common response. *Limnol. Oceanogr.* **39**, 1979–1984.

Witter, A.E., Hutchins, D.A., Butler, A., Luther, G.W., 2000a. Determination of conditional stability constants and kinetic con-

stants for strong model Fe-binding ligands in seawater. *Mar. Chem.* **69**, 1–17.

Witter, A.E., Lewis, B.L., Luther, G.W., 2000b. Iron speciation in the Arabian Sea. *Deep Sea Res. II* **47**, 1517–1539.

Witter, A.E., Luther, G.W., 1998. Variation in Fe-organic complexation with depth in the northwestern Atlantic Ocean as determined using a kinetic approach. *Mar. Chem.* **62**, 241–258.

Wu, J.F., Luther, G.W., 1995. Complexation of Fe(III) by natural organic-ligands in the northwest Atlantic Ocean by a competitive ligand equilibration method and a kinetic approach. *Mar. Chem.* **50**, 159–177.

Xiao, C.B., Palmer, D.A., Wesolowski, D.J., Lovitz, S.B., King, D.W., 2002. Carbon dioxide effects on luminol and 1,10-phenanthroline chemiluminescence. *Anal. Chem.* **74**, 2210–2216.